Langmuir

Article

A Ternary System Based on Fluorophore-Surfactant assemblies-Cu2+ for Highly Sensitive and Selective Detection of Arginine in Aqueous Solution

Jianhua Cao, Liping Ding, Wenting Hu, Xiangli Chen, Xiao Chen, and Yu Fang

Langmuir, **Just Accepted Manuscript** • DOI: 10.1021/la5039798 • Publication Date (Web): 02 Dec 2014

A Ternary System Based on Fluorophore-Surfactant assemblies-Cu^{2+} for Highly Sensitive and Selective Detection of Arginine in Aqueous Solution

Jianhua Cao, Liping Ding, Wenting Hu, Xiangli Chen, Xiao Chen, Yu Fang*

Key Laboratory of Applied Surface and Colloid Chemistry of Ministry of Education, School of Chemistry and Chemical Engineering, Shaanxi Normal University, Xi'an 710062, P. R. China

KEYWORDS. Dansyl, fluorescent sensor, amino acids, copper, supramolecular assemblies

ABSTRACT. A new cationic dansyl derivative-based (DIlSD) fluorescence probe was designed and synthesized. Its combination with anionic surfactant SDS assemblies shows enhanced fluorescence intensity and blue-shifted maximum wavelength. Its fluorescence can be slightly quenched by Cu^{2+}, however, the fluorescence quenching efficiency by Cu^{2+} is highly increased upon titration of arginine (Arg). As a result, the ternary system containing the cationic fluorophore, anionic surfactant, and Cu^{2+} function as a highly sensitive and selective sensor to Arg. The optimized sensor system displays a detection limit of 170 nM, representing the highest sensitivity to Arg in total aqueous solution by a fluorescent sensor. Control experiments reveal that the imidazolium groups in the fluorophore, the anionic surfactant, and Cu^{2+} all play important roles in the process of sensing Arg. The electrostatic interaction between the cationic fluorophore and anionic surfactants facilitates the binding of imidazolium rings with Cu^{2+}, the

surfactants surface-anchored Cu^{2+} is responsible for further binding of Arg, and the electrostatic interaction between anionic surfactants and positively charged amino acids accounts for the selective responses to Arg.

INTRODUCTION

Amino acids are the basic units of biological macromolecular proteins, and are also the essential components of life processes. Detection of amino acids is highly demanded in various fields such as nutritional analysis and medical diagnosis of diseases (e.g., Alzheimer and pancreatitis).[1] A great number of methods have been reported to detect various amino acids, which include chromatographic,[2] electrochemical,[3] and spectroscopic approaches[4,5]. By comparison, fluorescent chemosensors possess several advantages such as high sensitivity, high selectivity, easy operation, and real time or online detection.[6] Therefore, fluorescent sensors for amino acids have attracted great attention in recent years.

For example, Feng et al. reported that BINOL displayed on-off fluorescence responses to Cu^{2+}; in the process, BINOL was oxidized to dibenzo[a,kl]xanthen-1-ol. This oxidized fluorescent probe showed selective turn-on fluorescence responses to thiol-containing cysteine (Cys), homocysteine (Hcy), and glutathione (GSH) against other amino acids in acetonitrile/water.[7] Yang et al. synthesized a ratiometric fluorescent sensor based on monochlorinated BODIPY for highly selective detection of GSH over Cys and Hcy in acetonitrile/HEPES buffer.[8] Wang and coworkers reported using a coumarin-derived complex, Hg_2L_2, as a highly sensitive and selective probe for the detection of Cys in DMSO/H_2O.[9] Zhu et al. designed a chiral polymer and found its *in situ* complex with Zn^{2+} could function as a fluorescent sensor for highly enantioselective recognition of N-Boc-protected alanine in THF.[10]

However, instead of using pure aqueous solutions, many of the reported fluorescent sensors for amino acids are used in organic solvent-water mixtures.[11-13] Moreover, the types of amino acids that can be detected by fluorescent sensors are still limited. For example, fluorescent sensors for arginine are rarely reported. Therefore, developing simple, efficient, and inexpensive probes for the fluorescent recognition of more types of amino acids in total aqueous solution is highly desirable.

Amphiphilic surfactant molecules can form heterogeneous supramolecular assemblies in aqueous solutions, such as premicelles and micelles.[14] The hydrophobic domain formed by the hydrocarbon tails of surfactants can be used to encapsulate organic fluorophore. This strategy has been widely used in developing aqueous fluorescent sensors for various analytes, namely metal ions like Cu^{2+}, Hg^{2+}, and Cd^{2+}, etc.,[15-17] explosives,[18,19] and proteins[20,21]. However, this strategy for preparing fluorescent sensors for amino acids has been rarely reported.

In the present work, we designed and prepared a cationic dansyl-based fluorophore containing imidazolium group and combined it with anionic surfactant assemblies and Cu^{2+} to function as an aqueous fluorescent sensor for amino acids. Fluorescence studies reveal that the fluorophore/SDS/Cu^{2+} assemblies exhibit high sensitivity and selectivity toward arginine (Arg). To the best of our knowledge, there have been no reports on using surfactant assemblies to fabricate fluorescent sensors for Arg. The specific binding of fluorophore/SDS/Cu^{2+} to arginine leads to highly selective quenching of the SDS aggregation encapsulated fluorophore, allowing sensitive detection of arginine with a detection limit of 170 nM.

EXPERIMENTAL SECTION

Reagents and Instruments

Dansyl chloride (98%), bromoacetyl bromide (99%), diethylenetriamine (DETA, 98%), trifluoro acetic acid (99%), phenyl tert-butyl carbonate (98%), sodium dodecyl sulfate (SDS, >99%), decyltrimethylammonium bromide (DTAB, >98%), Triton X-100 (TX100), all the amino acids including L-arginine (Arg, 99%), L-glutamic acid (Glu, 99%), D-aspartic acid (Asp, 99%), L-lysine (Lys, 99%), cysteine (Cys, 99%), glycine (Gly, 99%), L-threonine (Thr, 99%), L-serine (Ser, 99%), L-alanine (Ala, 99%), L-proline (Pro, 99%), L-leucine (Leu, 99%), L-tryptophan (Try, 99%), and L-histidine (His, 98%), HEPES (>99.5%) and 1-methyl imidazole (>99%) were all purchased from Sigma-Aldrich company and used without further purification.

Melting point was measured on Microscopic Melting Point Meter (Beijing Tech Instrument). The ^{1}H NMR and ^{13}C NMR spectra of the synthesized chemicals were obtained on a Bruker Avance 400 MHz NMR spectrometer. The FTIR spectra were measured on a Fourier Transform Infrared Spectrometer (Vertex 70v, Bruker, Germany). The high resolution mass spectra (MS) were acquired in ESI positive mode using a Bruker Maxis UHR-TOF Mass Spectrometer. Fluorescence measurements were conducted at room temperature on a time-correlated single photon counting fluorescence spectrometer (Edinburgh Instruments FLS 920). UV-vis absorption spectra were recorded on a spectrophotometer (Lambda 950, Perkin-Elmer, USA).

Synthesis of the target imidazolium-derived dansyl-based fluorophore, DIlSD

The synthesis process of the target cationic dansyl-based fluorophore, namely DIlSD, from the commercially available starting materials is illustrated in Scheme 1. To obtain this target compound, several internal compounds including DETAB, DBSD, and DBrSD were needed to be first synthesized. DETAB was synthesized according to a patent method,[22] and used directly for the synthesis of DBSD. The detailed synthesis procedures of DBSD, DBrSD, and the target DIlSD are provided as follows:

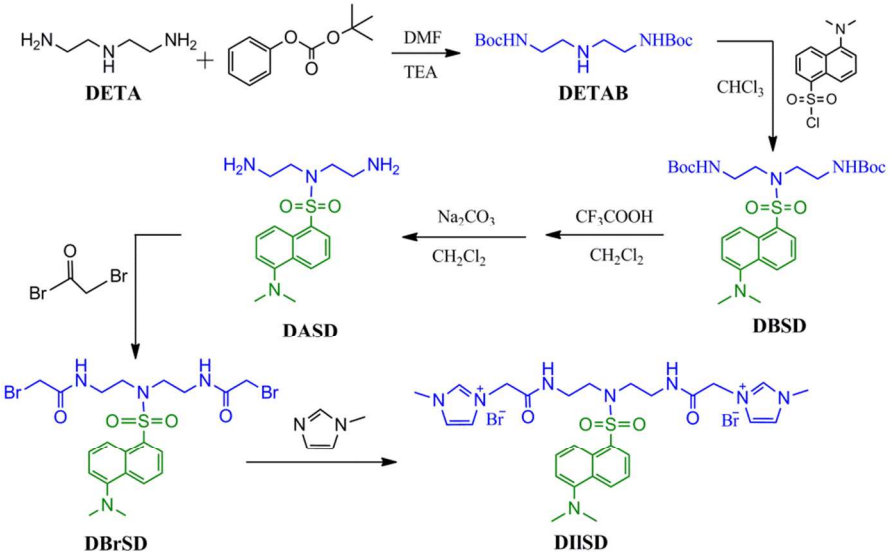

Scheme 1. Synthesis of bis-imidazolium derivative of dansyl-based fluorophore, DIlSD.

Synthesis of compound DBSD. DETAB (2.7 g, 9 mmol) was added to a stirred dry chloroform solution (70 mL) containing 2.7 g dansyl chloride (7 mmol). The reaction mixture was stirred for 12 h at room temperature, and the reaction process was monitored by thin layer chromatography (TLC). The solvent was evaporated and the residue was purified by column chromatography (hexane/ethyl acetate, v/v, 1:1) to afford DBSD as a yellow solid (1.6 g, yield 41%). ^{1}H-NMR (δ ppm, 400 MHz, $CDCl_3$): 8.54 (d, J = 8.0 Hz,1H), 8.27 (d, J = 8.0 Hz, 1H), 8.12 (d, J = 8.0 Hz, 1H), 7.56-7.48 (m, 2H), 7.17 (d, J = 8.0 Hz, 1H), 5.06 (s, 2H), 3.38-3.29 (m, 8H), 2.87 (s, 6H), 1.41 (s, 18H); ^{13}C NMR: (δ ppm, 101 MHz, $CDCl_3$): 156.05, 151.72, 134.39, 130.43, 130.00, 129.97, 129.29, 128.27, 123.11, 119.08, 115.20, 79.07, 48.36, 45.23, 39.41, 28.33 ppm; ESI-MS (m/z) ($C_{26}H_{40}N_4O_6S$): calculated [$(M+Na)^+$]: 559.2566, Found: 559.2560.

Synthesis of compound DASD. Trifluoroacetic acid (4.7 mL, 50 mmol) was dropped to the CH_2Cl_2 solution (9 mL) containing DBSD (0.4 g, 7 mmol). The resulting mixture was stirred overnight at room temperature. Then, the solvent was evaporated, and the residue was dissolved in 10 mL water. The aqueous layer was basified (pH ~ 9) with saturated sodium carbonate

solution and extracted with $CHCl_3$. The organic layers were combined and dried over anhydrous Na_2SO_4 overnight, filtered, and concentrated in vacuo to afford yellow oil DASD, which was used directly for the next step reaction.

Synthesis of compound DBrSD. DASD (0.25 g, 7 mmol) and triethylamine (0.4 mL) was dissolved in CH_2Cl_2 (50 mL) at 0 °C. A solution of bromoacetyl bromide (0.24 mL, 28 mmol) in CH_2Cl_2 (12 mL) was added dropwise to the cooled solution for about 30 min. Then the reaction mixture was stirred at room temperature for about 2 d. The reaction progress was monitored by TLC. Finally, the solution was washed with water (3 × 50 mL) and passed over anhydrous Na_2SO_4 and concentrated. The residue was purified by column chromatography (hexane/ethyl acetate, v/v, 1:3) to afford DBrSD as a yellow solid (0.25 g, yield: 62.5%). ^{1}H-NMR (δ ppm, 400 MHz, $CDCl_3$): 8.57 (d, J = 8.0 Hz, 1H), 8.19 (d, J = 8.6 Hz, 1H), 8.09 (d, J = 8.0 Hz, 1H), 7.57 - 7.50 (m, 2H), 7.20 (d, J = 8.0 Hz, 3H), 3.74 (s, 4H), 3.46 (s, 8H), 2.89 (s, 6H); ^{13}C NMR (δ ppm, 101 MHz, $CDCl_3$): 166.86, 151.72, 133.99, 131.11, 130.03, 129.90, 129.79, 128.57, 123.55, 119.33, 115.60, 47.85, 45.46, 39.13, 28.85; EMS-MS (m/z) ($C_{20}H_{26}Br_2N_4O_4S$): calculated [$(M+Na)^+$]: 600.9919, Found: 600.9911.

Synthesis of the target compound, DIlSD. DBrSD (0.25 g, 0.4 mmol) and methylimidazole (0.14 mL, 1.6 mmol) was dissolved in THF (50 mL). The resulting solution was refluxed for 2.5 d under nitrogen. The reaction process was monitored by TLC. At last, the reaction solution was filtered, and the left solid was heated in acetone under reflux for 8 h, filtered, and washed with ether to afford the title compound as a yellow solid (0.15 g, yield 65.2%). m.p.: 134.5 ~ 136.8 °C. ^{1}H NMR (δ ppm, 400 MHz, $CDCl_3$): 9.13 (s, 2H), 8.78 (t, J = 8.0 Hz, 2H), 8.50 (d, J = 8.0 Hz, 1H), 8.15 (d, J = 8.6 Hz, 1H), 8.04 (d, J = 8.0 Hz, 1H), 7.67-7.62 (m, 4H), 7.28 (d, J = 8.0 Hz, 1H), 4.98 (s, 4H), 3.90 (s, 6H), 3.42 (t, J = 8.0 Hz, 4H), 3.31 (t, J = 8.0 Hz, 4H), 2.83 (s,

6H); ^{13}C NMR: (δ ppm, 101 MHz, DMSO): 165.23, 151.48, 137.65, 134.65, 129.86, 129.27, 128.25, 127.96, 123.74, 123.63, 123.01, 118.67, 115.29, 50.48, 47.19, 44.92, 38.06, 35.90; IR (KBr) ν_{max} (cm^{-1}): 3405 (-NH), 3046 (Ar-H), 1623 (C=O), 1589 (C=N), 1318 (C-N), 1060 (S-N); ESI-MS (m/z) ($C_{28}H_{38}N_8O_4S^{2+}Br^-_2$): calculated [((M/2)-Br)$^+$]: 291.1366, Found: 291.1366.

Preparation of samples

The stock aqueous buffer solution of HEPES (200 mM, pH 7.4) were prepared by dissolving HEPES solid into water and adjusted by NaOH (1.0 M) to obtain the physiological pH. The stock solutions of DIlSD were prepared in water with a concentration at 0.25 mM. The stock solutions of amino acids (2.5 mM) and those of various metal ion salts (2.5 mM) were also prepared in water. The aqueous stock solutions of SDS (20 mM), DTAB (40 mM), and TX100 (1.0 mM) were prepared in water, and diluted to prepare the aqueous solutions of these surfactants at various concentrations. All aqueous solutions were prepared from Milli-Q water (18.2 MΩ cm at 25 °C).

The samples of aqueous solutions of DIlSD (10 μM) for all kinds of measurements were prepared in 10 mM HEPES buffer solutions (pH 7.4), where the appropriate amount of the stock solutions of DIlSD and HEPES were first mixed and then diluted by water, or the necessary surfactant aqueous solutions.

Fluorescence titration measurements

To a 3.5 mL quartz cuvette containing 2.5 mL testing solution in HEPES buffer (10 mM, pH 7.4), proper amounts of the examined analyte solutions were added with a micropipette and the resulting solution was stirred by a capillary tube. After this, the fluorescence spectra were measured with the excitation wavelength at 350 nm.

RESULTS AND DISCUSSION

Studies on the basic photophysical properties of DIlSD

The steady-state fluorescence emission of DIlSD (10 μM) was measured in different aqueous media that include only water, SDS (10 mM), DTAB (16 mM), and TX100 (0.5 mM), where all the solutions were prepared in HEPES buffer (10 mM, pH 7.4). The surfactant concentration was controlled above their corresponding critical micelle concentration (CMC). Interestingly, this cationic fluorophore shows very stable fluorescence emission either in water or in all the surfactant aqueous solutions (Figure S1, Supporting Information, SI). The surprising stability of the cationic fluorophore in water reveals that the fluorophore can be well dissolved in water. The fluorescence emission spectra in these media are shown in Figure 1a. Clearly, the fluorescence intensity of DIlSD is greatly enhanced in the presence of SDS micelles. The maximum emission wavelength is also blue-shifted from 564 nm in neat water to 537 nm in SDS solution. However, both the fluorescence intensity and the maximum emission do not apparently vary either in DTAB or in TX100 solution. The exposure to UV light (365 nm) reveals bright fluorescence emission only from SDS aqueous solution. The other two surfactant solutions exhibit similar dark emission as that in neat water. Dansyl moiety is a well-known polarity-sensitive probe and its maximum emission usually blue-shifts and the intensity increases along decreasing polarity of its surroundings.[23-25] Thus, the decreased polarity around dansyl moieties in SDS micellar solution suggests that the fluorescent probe is successfully encapsulated in the hydrophobic core of SDS micelles, where the hydrophobic interaction between dansyl moieties and SDS micelles should play a role. Moreover, the only encapsulating into SDS micelles rather than into DTAB and TX100 micelles also indicate that the electrostatic interaction between fluorophore and surfactant plays an important role in encapsulating the cationic fluorophores in the surfactant assemblies. The encapsulation in SDS assemblies also significantly increases the fluorescence

quantum yield of the fluorophore from 2.1% in water to 9.5% in SDS aqueous solution. However, the quantum yield is not increased either in TX100 (2.4%) or DTAB (2.2%) aqueous solutions.

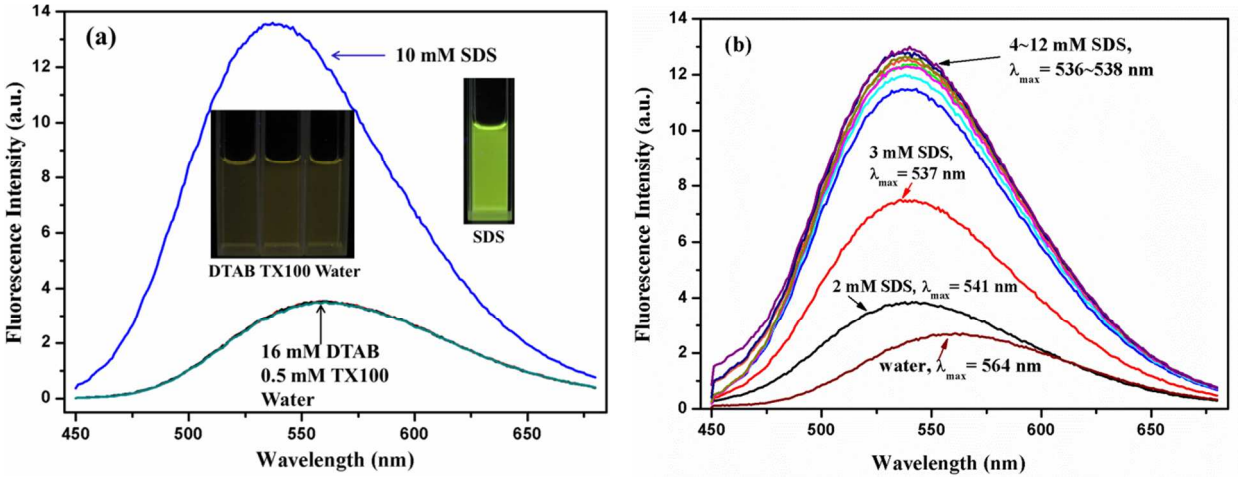

Figure 1. (a) Fluorescence emission spectra of DIlSD (10 μM) in water, SDS, DTAB, and TX100 aqueous solutions (10 mM HEPES, pH 7.4). (b) Fluorescence emission spectra of DIlSD (10 μM) in water and different concentrated SDS aqueous solution (10 mM HEPES, pH 7.4). (λex = 350 nm)

We also examined the concentration effect of SDS on the fluorescence emission of the probe. As observed in water, the cationic fluorophore shows stable fluorescence emission in all the tested SDS aqueous solutions (Figure S2 in the SI). Figure 1b illustrates the fluorescence emission spectra of the cationic fluorophore in different concentrated SDS aqueous solutions (10 mM HEPES, pH 7.4). Clearly, the increasing concentration of SDS from 2 to 4 mM leads to notable enhancement of fluorescence intensity and blue-shift of the maximum emission wavelength, indicating the polarity of the microenviroments surrounding the fluorophore in the SDS aggregations decreases. Such results suggest that SDS molecules over the range of 2~4 mM may already form some aggregates and provide hydrophobic microdomains for the cationic

fluorophore. Interestingly, further increasing SDS concentration from 4 to 12 mM does not bring much change either in the intensity or the maximum wavelength, revealing that the microdomain polarity of SDS aggregations is similar when SDS concentration is above 4 mM in HEPES buffer solution.

DIlSD/SDS/Cu^{2+} assemblies as sensor platform for Arg in aqueous solution

Considering copper ion is a universal quenching ion and imidazolium group can bind with Cu^{2+},[26,27] we intended to add Cu^{2+} to the aqueous solutions containing DIlSD to quench the fluorescence emission. Then, some amino acids that can bind Cu^{2+} ions may be able to turn on the Cu^{2+}-quenched fluorescence such as Gly[28] and Cys[7]. As a result, a turn on fluorescence sensor for amino acids may be obtained. However, the added Cu^{2+} (100 μM) did not produce much fluorescence variation of the cationic fluorophore (10 μM) in the aqueous buffer solution (Figure S3 in the SI). The reason for this could be due to the good solubility of the cationic fluorophore in aqueous solution. Thus, the two imidazolium groups are flexibly separated due to electrostatic repulsion, which is unfavorable for them to cooperate to bind with Cu^{2+}.

As previously reported, the negative SDS aggregations can attract Cu^{2+} ions and enhance fluorescence responses of the encapsulated fluorophore to the analytes.[15,28] Moreover, evidenced by the steady-state emission studies, the SDS aggregations can encapsulate the cationic fluorophore, which may shorten the distance between the two imidazolium groups and increase the chances of binding with Cu^{2+}. Therefore, we added Cu^{2+} to the aqueous buffer solution containing DIlSD/SDS ([DIlSD] = 10 μM; [SDS] = 4 mM). As expected, the addition of copper ions (35 μM) indeed caused some extent of quenching of the fluorescence emission of the sensor system. However, the further added amino acids did not cause any fluorescence recovery. On the contrary, one of the tested amino acids, Arg, induced further fluorescence quenching. As shown

in Figure 2a, the addition of 35 μM Cu^{2+} quenched ca. 11% of the original fluorescence emission. The gradual titration of Arg from 5 to 35 μM induced significant fluorescence quenching, where ca. 83% of the fluorescence emission was further quenched by the addition of 35 μM Arg in the presence of Cu^{2+}.

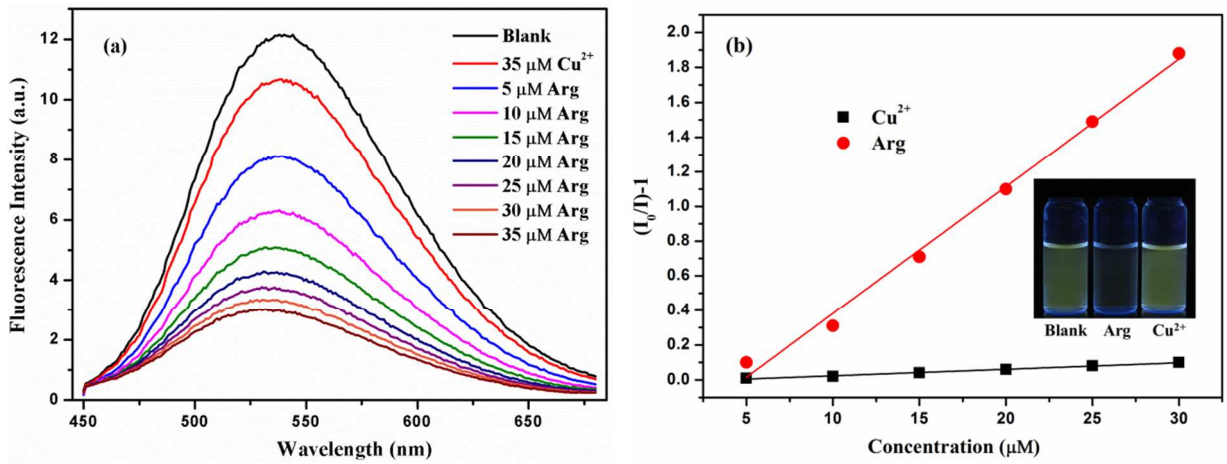

Figure 2. (a) Fluorescence emission spectra of DIlSD/SDS upon addition of Cu^{2+} (35 μM) and successive gradual addition of Arg in aqueous solution (10 mM HEPES, pH 7.4) (λex = 350 nm). (b) Fluorescence quenching of DIlSD/SDS/Cu^{2+} ([DIlSD] = 10 μM, [SDS] = 4 mM; [Cu^{2+}] = 35 μM) by Arg and further added Cu^{2+} (Inset: Photos of DIlSD/SDS/Cu^{2+} in the absence of quenchers and in the presence of 30 μM Arg and 30 μM Cu^{2+} upon illustration of 365 nm UV light).

However, further addition of Cu^{2+} to the 35 μM Cu^{2+}-quenched system produced much less fluorescence quenching. As shown in Figure S4 in the SI, the further addition of even 100 μM Cu^{2+} did not produce as much fluorescence quenching as observed for the addition of 35 μM Arg. The fluorescence quenching efficiency, (I_0/I)-1, was collected for both experiments and the results are shown in Figure 2b, where I_0 represent the maximum intensity of the fluorophore/SDS in the presence of 35 μM Cu^{2+}, and I represent the fluorescence intensity at the same wavelength upon addition of either Arg or extra Cu^{2+}. It can be seen that under the same experimental

condition, the addition of similar amount of Cu^{2+} produce much less fluorescence quenching than Arg. The exposure of the sensor system to UV light (365 nm) also discovered that the quenching by the addition of Arg leads to dark emission, whereas, the remaining fluorescence emission upon the addition of further more Cu^{2+} illustrates low quenching by Cu^{2+} (inset of Figure 2b).

We also checked the fluorescence responses of the sensor system to Arg in the absence of Cu^{2+} and found that the gradual addition of Arg even to 950 μM barely produced any fluorescence variation (Figure S5 in the SI). These results suggest that Cu^{2+} is the one that produces fluorescence quenching but with a low efficiency, and Arg is the one that facilitates the significant fluorescence quenching of the DIlSD/SDS assemblies by Cu^{2+}. Therefore, this Arg-facilitated fluorescence quenching may enable the fluorophore/SDS/Cu^{2+} system to function as a turn-off sensor for Arg. As we know, Arg is a very important type of amino acid and is involved in many important biological processes.[29-31] Therefore, many types of methods for detection of Arg have been exploited, which include visual detection based on gold nanoparticles,[29] radiochemical HPLC,[31,32] gas chromatography,[33] enzymatic end-point analysis,[34] electrochemical sensor,[35] and evanescent wave infrared chemical sensor,[36] etc. However, these methods either need sample pretreatment,[32] or involve several reaction steps,[34] or have low sensitivity[36]. This makes photoluminescent sensors are highly demanded in virtue of sensitivity and convenience[37]. However, the reported fluorescent and phosphorescent sensors for Arg are still very rare,[37-40] and some even have disadvantages such as detecting in organic solvents,[38] and low sensitivity[40]. Therefore, it is worthy to examine the sensing behavior of DIlSD/SDS/Cu^{2+} to amino acids in detail, to obtain highly sensitive and selective fluorescent sensor platform for aqueous detection of Arg, and to understand the sensing mechanism.

Concentration effect of Cu^{2+} and SDS on the sensing behavior of DIlSD/SDS/Cu^{2+} to Arg

To obtain the optimized sensor platform for Arg, the concentration effect of both Cu^{2+} and SDS on the sensing performance was examined. Firstly, the fluorescence responses of DIlSD/SDS/Cu^{2+} in HEPES buffer solution (10 mM, pH 7.4) toward Arg were investigated with different concentrations of Cu^{2+} (ranging from 5 μM to 40 μM), where the SDS concentration was fixed at 4 mM. For this measurement, a certain amount of Cu^{2+} was first added in the fluorophore/SDS system, and the maximum fluorescence intensity was recorded as I_0. Then, the stock aqueous solution of Arg was gradually added in the sensor system, and the fluorescence intensity at the same wavelength was recorded as I. The Stern-Volmer equation $I_0/I = 1 + K_{SV}$ was used to analyze the quenching kinetics of these sensor systems containing different concentrations of Cu^{2+}, where K_{SV} is the Stern-Volmer quenching constant and represents the sensitivity of the corresponding sensor system. As shown in Figure 3a, the concentration of Cu^{2+} could effectively influences the sensitivity of the sensor system to Arg. The highest sensitivity is observed in the presence of 25 μM of Cu^{2+}. Thus, the concentration of Cu^{2+} was controlled at 25 μM for the DIlSD/SDS/Cu^{2+} sensor system.

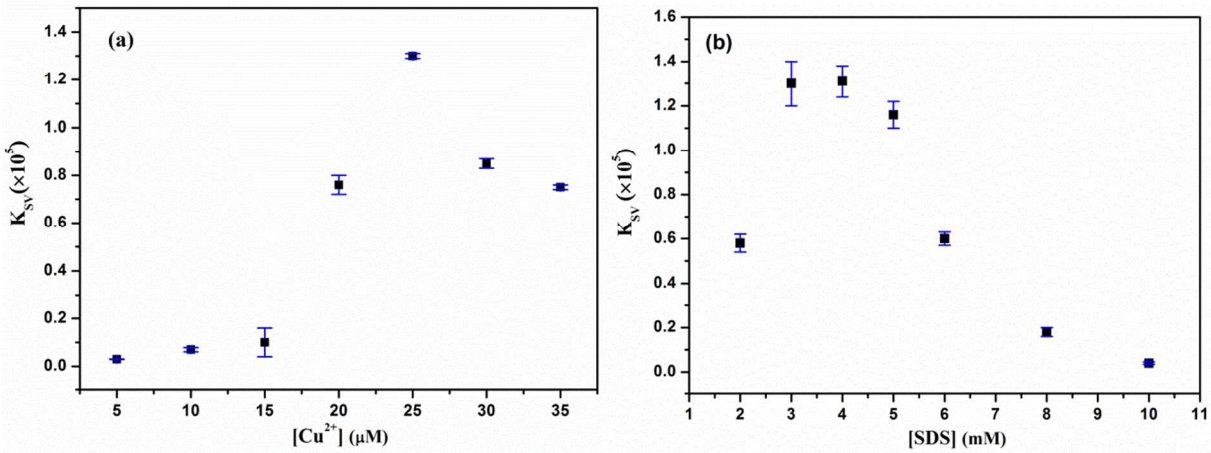

Figure 3. (a) Cu^{2+} concentration effect on the sensitivity of DIlSD/SDS/Cu^{2+} to Arg in HEPES buffer solution (10 mM, pH 7.4); (b) SDS concentration effect on the sensitivity of DIlSD/SDS/Cu^{2+} to Arg in HEPES buffer solution (10 mM, pH 7.4).

Then, the SDS concentration effect on the sensitivity to Arg was also measured. For this measurement, a series of DIlSD/SDS solutions containing different concentrations of SDS were first prepared. Then, 25 μM Cu^{2+} was added in these solutions to obtain a series of DIlSD/SDS/Cu^{2+} sensor systems, and the maximum fluorescence intensity was taken as I_0. After this, the aqueous stock solution of Arg was gradually titrated in the above solutions, and the fluorescence intensity at the same wavelength was recorded as I. Similarly, the K_{SV} values were determined from the slopes of plots of I_0/I of different sensor systems upon the concentration of Arg to evaluate their sensitivity. As shown in Figure 3b, the DIlSD/SDS/Cu^{2+} systems over a SDS concentration range of 3~5 mM possess a higher sensitivity than the other systems, and the one with 4 mM SDS exhibits the highest sensitivity. From the above results, we control SDS concentration at 4 mM and Cu^{2+} at 25 μM to obtain the optimized ternary sensor system and use it for the following studies. This ternary system was characterized by dynamic light scattering (DLS) and transmission electron microscopy (TEM). DLS revealed that the diameter of the aggregates is ca. 158.6 nm (Figure S6, SI). TEM images found similar diameter range of these aggregates (Figure S6, SI). These results suggest that the present ternary sensor system exist as micellar like aggregates.

Sensitivity and selectivity of DIlSD/SDS/Cu^{2+} sensor system to Arg

Sensitivity and selectivity are two of the most important characteristics of a sensor. Therefore, we systematically examined the sensitivity and selectivity of the optimized sensor system to Arg. Figure 4a illustrates the fluorescence emission variation upon addition of Arg from 2 to 80 μM. The fluorescence intensity of DIlSD/SDS/Cu^{2+} was taken as I_0, and the one in the presence of Arg was taken as I. The plot of $(I_0/I) - 1$ as a function of Arg concentration is illustrated in Figure 4b. Clearly, the plot is linearly increasing upon enlarging Arg concentration to 35 μM and

then reaches a plateau as Arg concentration is larger than 40 μM. The variation of $(I_0/I) - 1$ upon Arg concentration below 35 μM were repeatedly measured for three times and the results were shown in the inset of Figure 4b. The error bars represent the calculated standard deviation for three individual replicate measurements. Clearly, the linear relationship between $(I_0/I) - 1$ and Arg concentration below 35 μM follows the Stern-Volmer equation,

$$(I_0/I) - 1 = K_{SV}[\text{Arg}].$$

The K_{SV} value is determined to be 1.34×10^5 M^{-1}. This super large K_{SV} value represents a very high sensitivity to Arg. The detection limit is determined to be as low as 170 nM (c.f. SI for detailed determination process). As far as we know, this is the lowest detection limit that has been reported for detecting Arg using a fluorescent sensor (Table 1). We have also measured the fluorescence responses of this ternary system to D-arginine (D-Arg) and found that the sensor platform exhibits similarly remarkable fluorescence decreasing in the presence of D-Arg (Figure S7, SI). These results suggest that the prensent sensor can respond to both types of arginine, which makes it a specific sensor to arginine. The present work used L-arginine (Arg) as a representative of arginine.

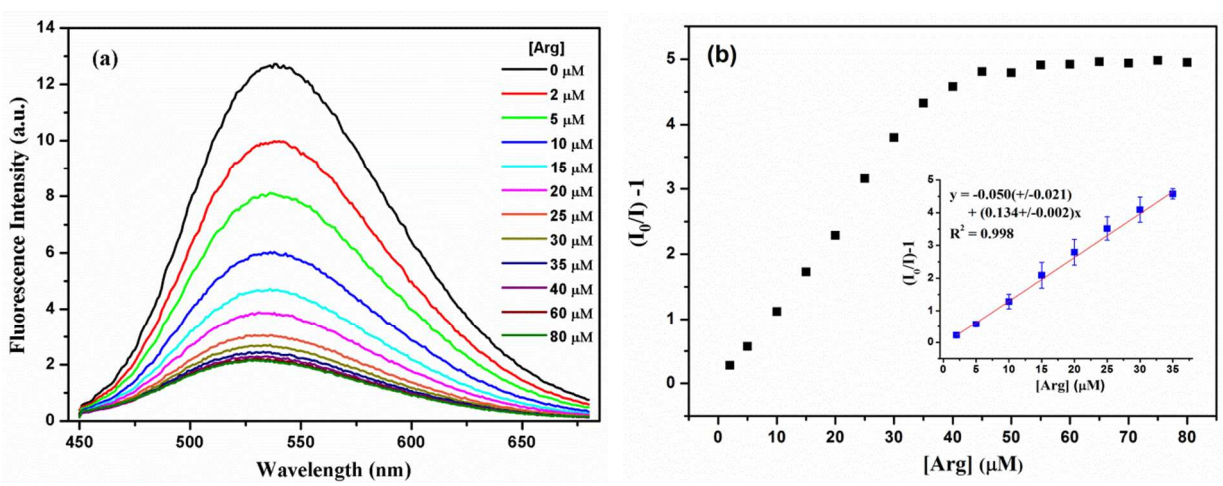

Figure 4. (a) Fluorescence emission spectra of DIlSD/SDS/Cu^{2+} sensor system upon titration of Arg in HEPES buffer solution (10 mM, pH 7.4) ([DIlSD] = 10 mM, [SDS] = 4 mM, λex = 350 nm). (b) Fluorescence intensity ratio, (I_0/I)-1, over the concentration of Arg, where I_0 and I stand for the fluorescence intensity of DIlSD/SDS/Cu^{2+} in the absence and presence of Arg, respectively (Inset: the linear relationship between (I_0/I)-1 and Arg concentration below 35 μM).

Table 1. Detection limit of Arg by various detection methods

Detection method	DL (μM)	Ref.
Fluorescent sensor	0.17	Present work
Fluorescent sensor	2.3	35
Fluorescent sensor	2.05	36
Fluorescent sensor	10	37
Phosphorescence sensor	0.23	38
Visual detection based on nanoparticles	0.016	29
Evanescent wave infrared chemical sensor	5	34
Electrochemical sensor	10	33

Then, the fluorescence responses of the sensor system to the other 12 amino acids were also measured. As shown in Figure 5, among all the other tested amino acids, only Lys could produce some extent fluorescence quenching. However, its quenching efficiency is determined to be 2.7×10^4 M^{-1}, much smaller than that of Arg. The detailed fluorescence responses of DIlSD/SDS/Cu^{2+} upon the titration of Lys and the determination of K_{SV} are provided in Figure S8 in the SI. The other 11 amino acids barely produce any fluorescence variation. When exposed to 365 nm UV light, the quenching of the green emission of the sensor system could only be visualized by the addition of 30 μM of Arg. It suggests that the present sensor system has a good selectivity to the presence of Arg and the detection of Arg could be visualized by using UV light exposure.

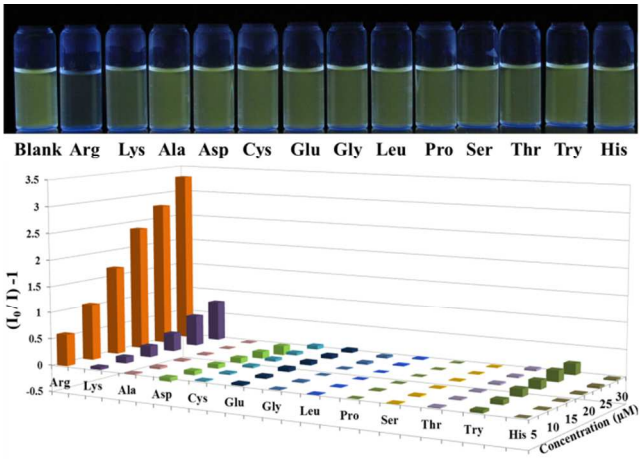

Figure 5. Top: Photos of DIlSD/SDS/Cu^{2+} in the absence and presence of various amino acids at 30 μM upon exposure to 365 nm UV light. Bottom: Fluorescence variation of DIlSD/SDS/Cu^{2+} upon addition of various amino acids from 5 to 30 μM ([DIlSD] = 10 μM; [SDS] = 4 mM; [Cu^{2+}] = 25 μM).

Sensing mechanism of DIlSD/SDS/Cu^{2+} to Arg

The present sensor system exhibits very interesting sensing performance to Arg. It is worthy to understand the sensing mechanism. Therefore, a series of control experiments were conducted to examine different factors that may influence the sensing process.

Firstly, we substituted Cu^{2+} in the sensor system with different metal ions to evaluate the role of Cu^{2+} or metal ions in the sensing process to Arg. Therefore, a series of metal ions (25 μM) were individually added to the DIlSD/SDS solutions to obtain various DIlSD/SDS/Metal-Ion systems. The responses of these sensor systems to the added Arg were measured and listed in Figure 6. It can be seen that unlike Cu^{2+}, the presence of all the other metal ions including Al^{3+}, Zn^{2+}, Fe^{3+}, Pb^{2+}, Hg^{2+}, Ba^{2+}, Mg^{2+}, Cd^{2+}, Ni^{2+}, and Co^{2+} did not induce responses of the DIlSD/SDS system to Arg. These results suggest that Cu^{2+} is the only critical metal ion that can enable the sensor system to respond to Arg. This could be due to two reasons: one is that Cu^{2+} could bind with both Arg[41,42] and imidazolium group[26,27], and the other is that Cu^{2+} is a

fluorescence quencher. It is known that Arg can also bind with Mg^{2+}.[37] The negative fluorescence responses of DIlSD/SDS/Mg^{2+} to Arg may be due to that Mg^{2+} does not produce fluorescence quenching. On the other hand, the slight responses to Arg in the presence of some quenching metal ions like Fe^{3+}, Ni^{2+}, and Co^{2+} may be attributed to the lack or weak binding of these metal ions with Arg and imidazolium group. This assumption is approved by UV-vis measurements. As illustrated in Figure S9 in the SI, the addition of Arg only produces variation of absorption of DIlSD/SDS in the presence of Cu^{2+}. For the systems with Mg^{2+}, Ni^{2+}, and Fe^{3+}, no apparent absorption changes are observed upon the titration of Arg, indicating slight binding between metal ions other than Cu^{2+} with Arg.

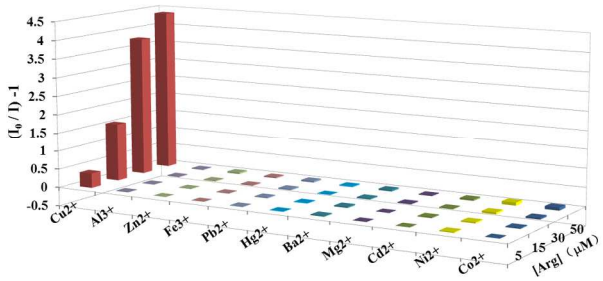

Figure 6. Fluorescence variation of DIlSD/SDS/M^{n+} (10 μM/4 mM/25 μM) in HEPES buffer solution (10 mM, pH 7.4) upon the titration of Arg. Note: M^{n+} refers to various metal ions listed in the figure.

Secondly, we examined the surfactant charge effect on the sensing process to Arg by substituting SDS in the DIlSD/SDS/Cu^{2+} system with cationic surfactant DTAB and neutral TX100. The results are shown in Figure 7. Clearly, the substitution of SDS with DTAB and TX100 in the sensor system leads to inert responses to Arg. Moreover, the absence of SDS also leads to none responses to Arg even in the presence of Cu^{2+} (Figure S10 in the SI). As shown in the inset of Figure 7, the exposure to UV light revealed that the sensor system with either DTAB or TX100 is more like the one in the water absence of surfactants. These results suggest that the

presence of anionic surfactant is also critical for DIlSD/SDS/Cu^{2+} sensing to Arg. The negative surfactant may play multiple roles in the present sensor platform. On one hand, it forms assemblies with the cationic fluorophore and shortens the distance between the two imidazolium groups and enables them to bind with Cu^{2+} to cause fluorescence quenching; on the other hand, its negative surface charges can attract Cu^{2+} through electrostatic interaction and enhances the local concentration of Cu^{2+},[15] and as a result, increases the chances of Cu^{2+} binding with amino acids.

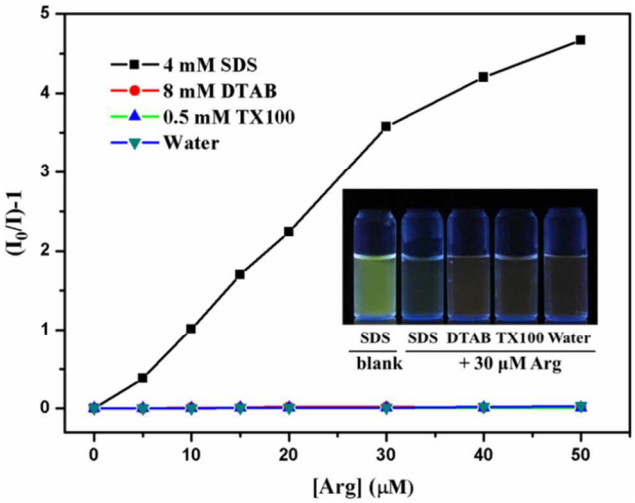

Figure 7. Fluorescence variation of DIlSD in different surfactant solutions in the presence of 25 μM Cu^{2+} upon addition of Arg. Inset: Photos of the solutions under 365 nm UV light.

We also investigated the role of imidazolium group in the fluorophore in the sensing to Arg. Therefore, we substituted DIlSD in the sensor system with DBrSD and measured the fluorescence responses of this new system to Arg. As illustrated in Figure S11a in the SI, the dansyl derivative without imidazolium shows no responses to Arg under the same testing condition. Moreover, its fluorescence can not be as quenched by Cu^{2+} (Figure S11b, SI) as that of DIlSD in SDS aqueous solution (Figure S4, SI), suggesting the binding with Cu^{2+} occurs for DIlSD rather than DBrSD. UV-vis measurements also reveal slight variation of absorbance of

DBrSD upon the addition of Cu^{2+} to the solution of DBrSD/SDS and the further addition of Arg (Figure S11c in the SI). These differences between DIlSD and DBrSD systems indicate that the imidazolium group in DIlSD is an essential unit for the fluorophore to function as a sensor to Arg, which empowers the fluorophore to both electrostatically interact with SDS assemblies and to bind with Cu^{2+}. The binding of imidazolium unit with Cu^{2+} probably comes from the N atom that is connected with methyl group.[43]

Based on the above results and discussion, we proposed a possible mechanism for the DIlSD/SDS/Cu^{2+} sensing Arg (Scheme 2). Firstly, the cationic fluorophore assembles with the anionic surfactant SDS aggregations through the electrostatic interaction between imidazolium group and sulfate group. Then, the two imidazolium units are close enough to bind with Cu^{2+} attracted by the negative surface of SDS aggregation, which leads to some fluorescence quenching. However, the two imidazolium groups in the fluorophore provide only two binding sites for Cu^{2+}, which renders a weak fluorophore-Cu^{2+} complex since a stable copper complex usually needs 4 binding ligands.[44,45] This may be the reason why the presence of Cu^{2+} alone leads to a very low quenching efficiency to the fluorophore. The addition of Arg, which can bind with Cu^{2+} and provide two more binding sites through its amino and carboxylic groups,[6,41] enables the bisimidazolium fluorophore, copper ion, and Arg to form a more stable sandwich structure, which leads to enhanced fluorescence quenching of Cu^{2+} to the fluorophore.

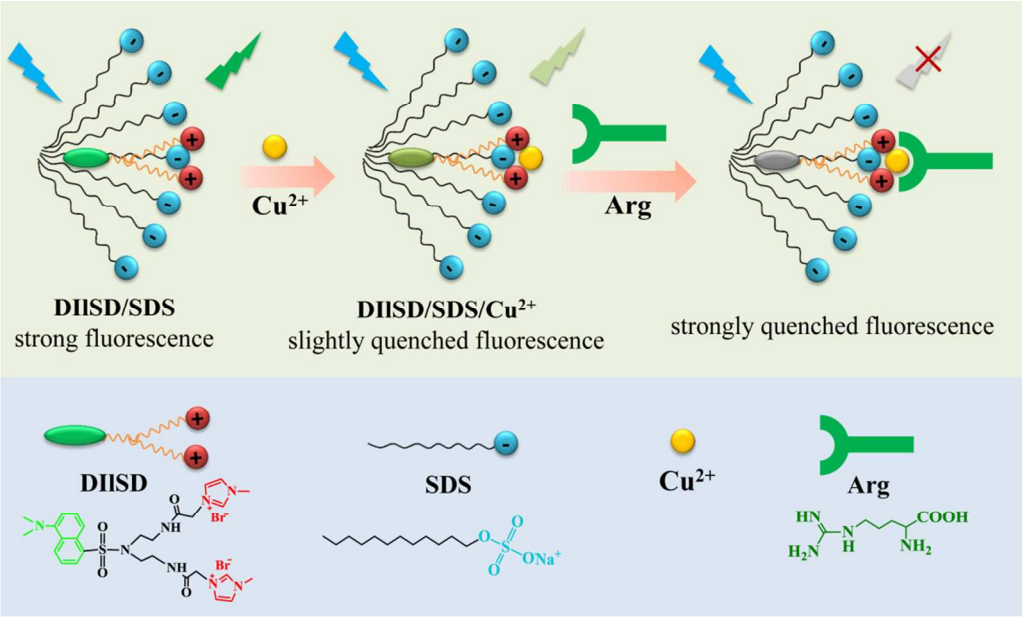

Scheme 2. Schematic representation of the sensing process of DIISD/SDS/Cu^{2+} to Arg.

However, it is known that besides Arg, Cu^{2+} could also bind with several other amino acids such as Cys, Asp, Glu, and His.[42,46] Then, why does the sensor system only selectively and sensitively response to Arg? This may be due to the different charges carried by the side chain of these amino acids at the physiological pH 7.4. It is known that Arg and Lys are basic amino acid (pI is 10.76 for Arg and 9.47 for Lys) and carries positive charge at pH 7.4.[47] The pI value for His is 7.64, leading to much less positive charges carried by His at pH 7.4.[47] Moreover, Asp, Glu, and Cys possess negative charges at pH 7.4 as their pI values are 2.77~2.98, 3.08~3.22, and 5.15, respectively.[47,48] Thus, as a result, only Arg and Lys can be electrostatically attracted to the negative surfaces of SDS aggregations, forms complex with Cu^{2+}, and enhances the quenching efficiency of copper ions to the SDS aggregation-encapsulated fluorophores, which agrees with the results shown in Figure 5. These results indicate that SDS aggregation plays a third role in sensing Arg, which is attracting positively charged amino acids through electrostatic interaction, which is the key factor determining the selectivity toward Arg. The larger pI value of Arg may

be responsible for the higher sensitivity to Arg than to Lys, which enables Arg carries more positive charges at pH 7.4.

We then measured the fluorescence responses of the present ternary sensor system to Arg in a biological matrix, namely, bovine serum solution, to check its potential application for biological samples. Bovine serum was dilluted 500-fold with HEPES (10 mM, pH 7.4) buffer before detection. The sensor system can still respond to Arg although with a smaller sensitivity compared to in aqueous solution (Figure S12a, SI). Moreover, the selectivity to Arg is also retained when measured in serum solution (Figure S12b, SI). This suggests that our method can be possibly applied to biological samples.

CONCLUSION

The ternary system containing the cationic imidazolium-derived dansyl fluorophore, anionic SDS assemblies, and Cu^{2+} exhibits high sensitivity and selectivity towards Arg among the 13 tested amino acids. Control experiments reveal that the absence of either the imidazolium group in the fluorophore, or the negative surfactant, or Cu^{2+} leads to inert responses of the ternary system to Arg, approving the necessity of the three components in the sensor system in realization of the selective and sensitive recognition of Arg. The electrostatic interaction between the cationic fluorophore and the anionic surfactant assemblies enables the two imidazolium rings in near vicinity to bind Cu^{2+}. The imidazolium ring anchored Cu^{2+} ions then function both as a bridge to further bind amino acids and as a quencher to the fluorophore emission. Moreover, the negative surface of the supramolecular assemblies empowers the anchored Cu^{2+} ions to selectively bind with the positively charged Arg at physiological pH. The present work, on one hand, enlarges the scope of analytes of surfactant assemblies-based fluorescent sensors, and on the other hand, realizes the highly sensitive and selective detection of Arg in organic-solvent-free,

total aqueous solution with a detection limit of 170 nM. Moreover, this method does not need pre-sample treatment and the reponse is fast, which makes the present method a fast and convenient way to detect arginine.

ASSOCIATED CONTENT

Supporting Information. Fluorescence quantum yield measurements, determination of detection limit to Arg, fluorescence stability of DIlSD in various media, fluorescence responses of various control systems to Cu^{2+} or Arg, fluorescence responses of DIlSD/SDS/Cu^{2+} to Lys, UV-vis absorption of DIlSD/SDS/M^{n+} to Arg, and fluorescence and UV-vis absorption responses of DBrSD/SDS/Cu^{2+} to Arg. This material is available free of charge via the Internet at http://pubs.acs.org.

AUTHOR INFORMATION

Corresponding Author

*E-mail: dinglp33@snnu.edu.cn; Tel: 86-29-8153-0789 (O)

Notes

The authors declare no competing financial interest.

ACKNOWLEDGMENT

The authors acknowledge the financial support from National Natural Science Foundation of China (21173142), Ministry of Education of China (NCET-12-0895), Shaanxi Provincial Department of Science and Technology (2011KJXX48), the Program of Introducing Talents of Discipline to Universities (B14041), and the Fundamental Research Funds for the Central Universities (GK201301006).

REFERENCES

(1) Minami, T.; Esipenko, N. A.; Zhang, B.; Isaacs, L.; Pavel Anzenbacher, J. ‘‘Turn-on’’ Fluorescent Sensor Array for Basic Amino Acids in Water. *Chem. Commun.* **2014**, *50*, 61-63.

(2) Bhawani, S. A.; Ibrahim, M. N. M.; O. Sulaimanb, R. H.; Mohammad, A.; Hena, S. Thin-Layer Chromatography of Amino Acids: A Review. *J. Liq. Chromatogr. Relat. Technol.* **2012**, *35*, 1497-1516.

(3) Fu, Y.; Han, Q.; Chen, Q.; Wang, Y.; Zhou, J.; Zhang, Q. A New Strategy for Chiral Recognition of Amino Acids. *Chem. Commun.,* **2012**, *48*, 2322-2324.

(4) Mobarraz, M.; Ganjali, M. R.; Chaichi, M. J.; Norouzi, P. Functionalized Zns Quantum Dots as Luminescent Probes for Detection of Amino Acids. *Spectrochim. Acta, Part A* **2012**, *96*, 801–804.

(5) Buryak, A.; Severin, K. A Chemosensor Array for the Colorimetric Identification of 20 Natural Amino Acids. *J. Am. Chem. Soc.* **2005**, *127*, 3700-3701.

(6) Zhou, Y.; Yoon, J. Recent Progress in Fluorescent and Colorimetric Chemosensors for Detection of Amino Acids. *Chem. Soc. Rev.* **2012**, *41*, 52-67.

(7) Peng, R.; Lin, L.; Wu, X.; Liu, X.; Feng, X. Fluorescent Sensor Based on Binol for Recognition of Cysteine, Homocysteine, and Glutathione. *J. Org. Chem.* **2013**, *78*, 11602-11605.

(8) Niu, L.-Y.; Guan, Y.-S.; Chen, Y.-Z.; Wu, L.-Z.; Tung, C.-H.; Yang, Q.-Z. Bodipy-Based Ratiometric Fluorescent Sensor for Highly Selective Detection of Glutathione over Cysteine and Homocysteine. *J. Am. Chem. Soc.* **2012**, *134*, 18928-18931.

(9) Wu, J.; Sheng, R.; Liu, W.; Wang, P.; Ma, J.; Zhang, H.; Zhuang, X. Reversible Fluorescent Probe for Highly Selective and Sensitive Detection of Mercapto Biomolecules. *Inorg. Chem.* **2011**, *50*, 6543–6551.

(10) Hou, J.; Song, F.; Lu Wang, G. W.; Cheng, Y.; Zhu, C. In Situ Generated 1:1 Zn(Ii)-Containing Polymer Complex Sensor for Highly Enantioselective Recognition of N‑Boc-Protected Alanine. *Macromolecules* **2012**, *45*, 7835-7842.

(11) Kwon, H.; Lee, K.; Kim, H.-J. Coumarin–Malonitrile Conjugate as a Fluorescence Turn-on Probe for Biothiols and Its Cellular Expression. *Chem. Commun.* **2011**, *47*, 1773–1775.

(12) Zhou, Y.; Won, J.; Lee, J. Y.; Yoon, J. Studies Leading to the Development of a Highly Selective Colorimetric and Fluorescent Chemosensor for Lysine. *Chem. Commun.* **2011**, *47*, 1997-1999.

(13) Chen, X.; Ko, S.-K.; Kim, M. J.; Shin, I.; Yoon, J. A Thiol-Specific Fluorescent Probe and Its Application for Bioimaging. *Chem. Commun.* **2010**, *46*, 2751–2753.

(14) Ramanathan, M.; Shrestha, L. K.; Mori, T.; Ji, Q.; Hill, J. P.; Ariga, K. Amphiphile Nanoarchitectonics: From Basic Physical Chemistry to Advanced Applications. *Phys. Chem. Chem. Phys.* **2013**, *15*, 10580-10611.

(15) Mallick, A.; Mandal, M. C.; Haldar, B.; Chakrabarty, A.; Das, P.; Chattopadhyay, N. Surfactant-Induced Modulation of Fluorosensor Activity: A Simple Way to Maximize the Sensor Efficiency. *J. Am. Chem. Soc.* **2006**, *128*, 3126-3127.

(16) Avirah, R. R.; Jyothish, K.; Ramaiah, D. Dual-Mode Semisquaraine-Based Sensor for Selective Detection of Hg^{2+} in a Micellar Medium. *Org. Lett.,* **2007**, *9*, 121-124.

(17) Mameli, M.; Aragoni, M. C.; Arca, M.; Caltagirone, C.; Demartin, F.; Farruggia, G.; Filippo, G. D.; Devillanova, F. A.; Garau, A.; Isaia, F.; Lippolis, V.; Murgia, S.; Prodi, L.; Pintus, A.; Zaccheroni, N. A Selective, Nontoxic, Off–on Fluorescent Molecular Sensor Based on 8-Hydroxyquinoline for Probing Cd^{2+} in Living Cells. *Chem. Eur. J.* **2010**, *16*, 919-930.

(18) Hughes, A. D.; Glenn, I. C.; Patrick, A. D.; Ellington, A.; Anslyn, E. V. A Pattern Recognition Based Fluorescence Quenching Assay for the Detection and Identification of Nitrated Explosive Analytes. *Chem. Eur. J.* **2008**, *14*, 1822 –1827.

(19) Ding, L.; Bai, Y.; Cao, Y.; Ren, G.; Blanchard, G. J.; Fang, Y. Micelle-Induced Versatile Sensing Behavior of Bispyrene-Based Fluorescent Molecular Sensor for Picric Acid and Pyx Explosives. *Langmuir* **2014**, *30*, 7645-7653.

(20) Jia, L.; Xu, L.; Wang, Z.; Xu, J.; Ji, J. Label-Free Fluorescent Sensor for Probing Heparin-Protein Interaction Based on Supramolecular Assemblies. *Chin. J. Chem.* **2014**, *32*, 85-90.

(21) Azagarsamy, M. A.; Yesilyurt, V.; Thayumanavan, S. Disassembly of Dendritic Micellar Containers Due to Protein Binding. *J. Am. Chem. Soc.* **2010**, *132*, 4550-4551.

(22) Holmes, C. P.; Chakrabarti, A.; Ferederick, B. T.; Pan, Y.; Dong, Y. S.; Bhandari, A. Nitrogen-Based Linkers for Attaching Modifying Groups to Polypeptides and Other Macromolecules. U.S. Patent 8106154B2, Aug. 07, 2008.

(23) Hayashida, O.; Ogawa, N.; Uchiyama, M. Surface Recognition and Fluorescence Sensing of Histone by Dansyl-Appended Cyclophane-Based Resorcinarene Trimer. *J. Am. Chem. Soc.* **2007**, *129*, 13698-13705.

(24) Grieser, F.; Thistlethwaite, P.; Urquhart, R.; Patterson, L. K. Photophysical Behavior in Spread Monolayers. Dansyl Fluorescence as a Probe for Polarity at the Air-Water Interface. *J. Phys. Chem. B* **1987**, *91*, 5286-5291.

(25) Ghiggino, K. P.; Lee, A. G.; Meech, S. R.; O'Connor, D. V.; Phillips, D. Time-Resolved Emission Spectroscopy of the Dansyl Fluorescence Probe. *Biochemistry* **1981**, *20*, 5381-5389.

(26) Zheng, X.; Wang, M.; Sun, Z.; Chen, C.; Ma, J.; Xu, J. Preparation of Copper (Ii) Ion-Containing Bisimidazolium Ionic Liquid Bridged Periodic Mesoporous Organosilica and the Catalytic Decomposition of Cyclohexyl Hydroperoxide. *Catal. Commun.* **2012**, *29* 149-152.

(27) Zhang, X.; Tian, Y.; Li, Z.; Tian, X.; Sun, H.; Liu, H.; Moore, A.; Ran, C. Design and Synthesis of Curcumin Analogues for in Vivo Fluorescence Imaging and Inhibiting Copper-Induced Cross-Linking of Amyloid Beta Species in Alzheimer's Disease. *J. Am. Chem. Soc.* **2013**, *135*, 16397-16409.

(28) Ding, L.; Wang, S.; Liu, Y.; Cao, J.; Fang, Y. Bispyrene/Surfactant Assemblies as Fluorescent Sensor Platform: Detection and Identification of Cu^{2+} and Co^{2+} in Aqueous Solution. *J. Mater. Chem. A* **2013**, *1*, 8866–8875.

(29) Pu, W.; Zhao, H.; Huang, C.; Wu, L.; Xu, D. Visual Detection of Arginine Based on the Unique Guanidino Group-Induced Aggregation of Gold Nanoparticles. *Anal. Chim. Acta* **2013**, *764*, 78-83.

(30) Wu, G.; Bazer, F. W.; Davis, T. A.; Kim, S. W.; Li, P.; Rhoads, J. M.; Satterfield, M. C.; Smith, S. B.; Spencer, T. E.; Yin, Y. Arginine Metabolism and Nutrition in Growth, Health and Disease. *Amino Acids* **2009**, *37*, 153–168.

(31) Barilli, A.; Visigalli, R.; Rotoli, B. M.; Bussolati, O.; Gazzola, G. C.; Parolari, A.; Dall'Asta, V. Radiochemical High-Performance Liquid Chromatography Detection of Arginine Metabolism in Human Endothelial Cells. *Anal. Biochem.* **2012**, *424*, 156–161.
(32) Gopalakrishnan, V.; Burton, P. J.; Blaschke, T. F. High-Performance Liquid Chromatographic Assay for the Quantitation of L-Arginine in Human Plasma. *Anal. Chem.* **1996**, *68*, 3520-3523.
(33) Williams, A. Plasma-L-Arginine Levels in a Rabbit Model of Hypercholesterolemia. *Biochem. Pharmacol.* **1993**, *46*, 2097-2099.
(34) de Orduña, R. M. Quantitative Determination of L-Arginine by Enzymatic End-Point Analysis. *J. Agric. Food Chem.* **2001**, *49*, 549-552.
(35) Komaba, S.; Fujino, Y.; Matsuda, T.; Osaka, T.; Satoh, I. Biological Determination of Ag(I) Ion and Arginine by Using the Composite Film of Electroinactive Polypyrrole and Polyion Complex. *Sens. Actuators, B* **1998**, *52*, 78–83.
(36) Wei, Y. K.; Yang, J. Evanescent Wave Infrared Chemical Sensor Possessing a Sulfonated Sensing Phase for the Selective Detection of Arginine in Biological Fluids. *Talanta* **2007**, *71*, 2007-2014.
(37) Ren, H.-B.; Yan, X.-P. Ultrasonic Assisted Synthesis of Adenosine Triphosphate Capped Manganese-Doped Zns Quantum Dots for Selective Room Temperature Phosphorescence Detection of Arg and Methylated Arginine in Urine Based on Supramolecular Mg^{2+}-Adenosine Triphosphate–Arginine Ternary System. *Talanta* **2012**, *97*, 16-22.
(38) He, M.; So, V. L. L.; Xin, J. H. A New Rhodamine-Thiourea/Al^{3+} Complex Sensor for the Fast Visual Detection of Arginine in Aqueous Media. *Sens. Actuators, B* **2014**, *192*, 496-502.
(39) Zhou, X.; Jin, X.; Li, D.; Wu, X. Selective Detection of Zwitterionic Arginine with a New Zn(Ii)-Terpyridine Complex: Potential Application in Protein Labeling and Determinationw. *Chem. Commun.* **2011**, *47*, 3921–3923.
(40) Nasomphan, W.; Tangboriboonrat, P.; Smanmoo, S. Selective Sensing of L-Arginine Employing Luminol Dextran Conjugate. *Macromol. Res.* **2012**, *20*, 344-346.
(41) Binolfi, A.; Lamberto, G. R.; Duran, R.; Quintanar, L.; Bertoncini, C. W.; Souza, J. M.; Cerveñansky, C.; Zweckstetter, M.; Griesinger, C.; Fernández, C. O. Site-Specific Interactions of Cu(Ii) with A and B-Synuclein: Bridging the Molecular Gap between Metal Binding and Aggregation. *J. Am. Chem. Soc.* **2008**, *130*, 11801-11812.
(42) Miao, R.; Mu, L.; Zhang, H.; She, G.; Zhou, B.; Xu, H.; Wang, P.; Shi, W. Silicon Nanowire-Based Fluorescent Nanosensor for Complexed Cu^{2+} and Its Bioapplications. *Nano Lett.* **2014**, *14*, 3124-3129.
(43) Valderrama-Negrón, A. C.; Alves, W. A.; Cruz, Á. S.; Rogero, S. O.; Silva, D. d. O. Synthesis, Spectroscopic Characterization and Radiosensitizing Properties of Acetato-Bridged Copper(Ii) Complexes with 5-Nitroimidazole Drugs. *Inorg. Chim. Acta* **2011**, *367*, 85-92.
(44) Pramanik, A.; Basu, A.; Das, G. Coordination Assembly of P-Substituted Aryl Azo Imidazole Complexes: Influences of Electron Donating Substitution and Counter Ions. *Polyhedron* **2010**, *29*, 1980-1989.
(45) Molphy, Z.; Prisecaru, A.; Slator, C.; Barron, N.; McCann, M.; Colleran, J.; Chandran, D.; Gathergood, N.; Kellett, A. Copper Phenanthrene Oxidative Chemical Nucleases. *Inorg. Chem.* **2014**, *53*, 5392-5404.

(46) Chen, X.; Wong, C. K. Y.; Yuan, C. A.; Zhang, G. Impact of the Functional Group on the Working Range of Polyaniline as Carbon Dioxide Sensors. *Sens. Actuators, B* **2012**, *175*, 15-21.

(47) Liu, H. X.; Zhang, R. S.; Yao, X. J.; Liu, M. C.; Hu, Z. D.; Fan, B. T. Prediction of the Isoelectric Point of an Amino Acid Based on Ga-Pls and Svms. *J. Chem. Inf. Comput. Sci.* **2004**, *44*, 161-167.

(48) Righetti, P. G.; Gelfi, C.; Bossi, A.; Olivieri, E.; Castelletti, L.; Verzola, B.; Stoyanov, A. V. Capillary Electrophoresis of Peptides and Proteins in Isoelectric Buffers: An Update. *Electrophoresis* **2000**, *21*, 4046-4053.

TOC figure